ELSEVIER

0141-0296(95)00059-3

Engineering Structures, Vol. 18, No. 4, pp. 271-278, 1996

0141-0296/96 $15.00 + 0.00

Seismic analysis of towers including foundation uplift

Chaojin Xu and C. C. Spyrakos

Department of Civil Engineering, West Virginia University, Morgantown, WV 26506, USA
(Received October 1994; revised version accepted February 1995)

A seismic analysis procedure including soil-structure interaction and partial foundation uplift for tower structures is developed. The nonlinear equations of motion are derived with the aid of Lagrange's equation. Parametric studies are performed to evaluate the effects of factors such as: soil stiffness, ratio of tower height to foundation width, and partial separation of the foundation from the soil. The studies indicate that the effects of soil stiffness on a short tower are greater than on a slender one. The height-width ratio affects the seismic response of the tower significantly, especially for a tower at a rock-like location. The allowance of foundation uplift may substantially reduce the seismic response of moment and foundation rotation in the case of hard soil and a slender tower, or may greatly increase the seismic response of shear in the case of hard soil and a short tower. The study concludes that uplift is not always beneficial and its effects could be significant for structures under strong seismic motions.

Keywords: towers, seismic analysis, foundation uplift

1. Introduction

The seismic response of tall, slender structures such as piers, chimneys, and towers has attracted considerable attention. According to the assumptions on the bonding condition between the foundation and soil as well as the flexibility of the structure, the analytical approaches of treating the system can be divided into three categories where:

(1) It is assumed that the structure is rigid and is supported by a rigid soil base through gravity. Most studies have been limited to the overturning of objects such as furniture, equipment, and inverted pendulum-type systems. A review of the research on this subject has been presented by Ishiyama[1]. As early as 1881, West and Milne[2] developed a formula to calculate the critical ground acceleration which, when exceeded, leads to the overturning of rigid block structures. Motivated by the overturning behaviour of slender structures during the Chilean earthquake in 1960, Housner[3] studied the rocking motion of inverted pendulum structures. His studies showed that 'there is a scale effect which makes the larger of two geometrically similar blocks more stable than the smaller block'. Using a numerical procedure, Yim *et al.*[4] extended the analysis to rigid blocks subjected to earthquake ground motions. Spanos and Koh[5,6] in their research on the rocking motion of rigid blocks identified a stable region for the block in the form of the amplitude versus the frequency content of the excitation. It should be noted that the usefulness of results based on the assumption of rigid structure and soil is limited.

(2) In this category, the flexibility of the structure is incorporated in the analysis. Depending on the assumption adopted for the soil stiffness, the research can be divided into two approaches. The first approach postulates that the soil is rigid, and the second approach accounts for soil flexibility. Most early research followed the first approach, e.g., Housner[7]. Representative studies employing the second approach include the work of Luco[8], who used a substructure method to determine the response of a superstructure–foundation–soil system. Wolf[9], Spyrakos *et al.*[10–13], and Antes *et al.*[14] combined finite and boundary element methods to model the structure and soil interface, respectively. The studies in this category assume a complete bond between the foundation and the soil during the seismic excitation and ignore the effect of possible partial separation and sliding between the foundation and the soil.

(3) In the third category, foundation uplift is considered. Both the superstructure and the soil can be flexible. A comprehensive review of studies on foundations in bilateral and unilateral contact before 1988 has been presented by Spyrakos[11]. Psycharis and Jennings[15] studied the dynamic response of a rigid block which

was allowed to uplift. In their work they considered two models for the soil reactions: the Winkler foundation, and the much simpler two-spring foundation. To consider the beneficial effects of foundation uplift, Chopra and Yim[16] modelled a simple structure as a single-degree-of-freedom system with mass concentrated at the top. The soil was modelled with two springs and viscous dashpots placed at the foundation tips, thus permitting uplift but no sliding of the structure. Later they extended their analysis to multi-degree-of-freedom structures[17]. Adopting a two spring and dashpot idealization for the soil, Al-Deghaither[18] studied the dynamic response of a bridge pier which was allowed to uplift. Patel and Spyrakos[19,20] extended their previous work on FEM-BEM formulations to include uplift and sliding. The developments presented in their work allow treatment of elastodynamic problems involving partial loss of contact and sliding between elastic bodies as is exemplified through representative soil–structure interaction problems. Nonlinearities arising from soil–foundation separation and sliding are incorporated with interface finite elements.

In this study, an analytical procedure is developed to perform the seismic analysis of towers. The interaction of structure and soil is incorporated in the analysis. The tower is flexible and its deformation is expressed with assumed modes. Several low dynamic mode shapes of a cantilever beam are used as the assumed modes. Lagrange's equations are employed to derive the system's equation of motion. The interaction between the soil and the structure is simulated with a two spring–dashpot system which cannot support tension forces in order to account for partial separation of the foundation from the soil.

The nonlinear equations of motion are solved by Newmark's numerical integration method. The time steps of integration are of critical importance for the accuracy and efficiency of the method. Another factor that influences the accuracy of the solution is the number of assumed modes in the formulation. A convergence study has been performed to select the proper time step and number of assumed modes. Numerical examples are given to demonstrate the significance of the salient parameters in the system. These parameters include: soil stiffness, height-width ratio of the tower, and bond conditions.

The objectives of this work include the development of an analytical procedure that can be used to perform preliminary seismic analysis of towers in partial contact with their foundation and the assessment of the significance of foundation uplift, soil stiffness, and height-width ratio on the response of tall slender structures.

2. Formulation of the problem

The tower system shown in *Figure 1* consists of four parts: a top operation unit; a tall, slender tower; a rigid foundation; and the supporting soil. The operation unit with a mass of M_o is lumped at the top of the tower. The tower is idealized as a homogeneous isotropic tapered-beam structure with a distributed moment of inertia $I(x)$ and mass per unit length $m(x)$. The total mass of the tower is denoted as M_b. The tower is bonded to a rigid foundation block with zero height and radius R. The total mass of the foundation is denoted as M_f and its moment of inertia as I_f. The soil supporting the foundation is modelled by a two spring–

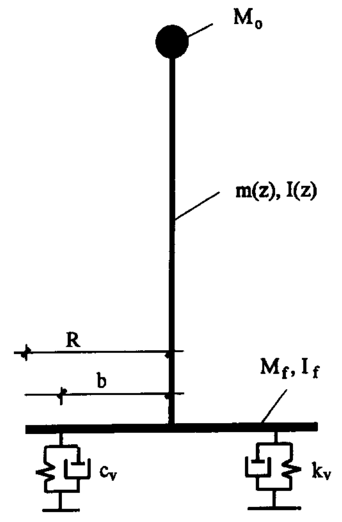

Figure 1 Simplified tower model

dashpot system as shown in *Figure 1*. Even though the stiffness and damping coefficients of the foundation–soil system are frequency dependent, in this study they are approximated by

$$K_z = \frac{4G_sR}{1-\nu_s} \tag{1}$$

$$K_\phi = \frac{8G_sR^3}{3(1-\nu_s)} \tag{2}$$

$$C_z = 0.85K_zR\left(\frac{\rho_s}{G_s}\right)^{\frac{1}{2}} \tag{3}$$

where K_z is the vertical stiffness, K_ϕ is the rocking stiffness, C_z is the vertical damping coefficient, G_s, ν_s, ρ_s are the shear modulus, Poisson's ratio, and mass density of the soil, respectively, and R is the radius of the circular foundation. In order to simulate the soil–foundation separation, the spring and dashpot are substituted by two springs and dashpots placed at the foundation tips a distance b apart. From equilibrium conditions b can be determined as[21]

$$b = \sqrt{\frac{2}{3}}R \tag{4}$$

The stiffness and damping coefficients for each spring–dashpot are given by

$$K_v = \frac{1}{2}K_z \qquad c_v = \frac{1}{2}c_z \tag{5}$$

This study considers only the response of the system to a horizontal ground motion, $\ddot{u}_g(t)$. Further, it is assumed that the frictional force between the foundation and the soil is large enough to prevent any horizontal slippage. The displacement and force configuration are shown in *Figure 2*, where $u(x,t)$ is the deflection of the tower and $\theta(t)$ is the rotation of the foundation. Prior to the earthquake ground excitation, the foundation rests on the spring–damper system through gravity and has an elastic vertical displacement of v_s, which remains constant until foundation uplift. The formulation is developed under the assumption of small displacements and rotation, and neglecting P–Δ effects[16,22]. The relative displacement $U(x,t)$ with respect to the ground

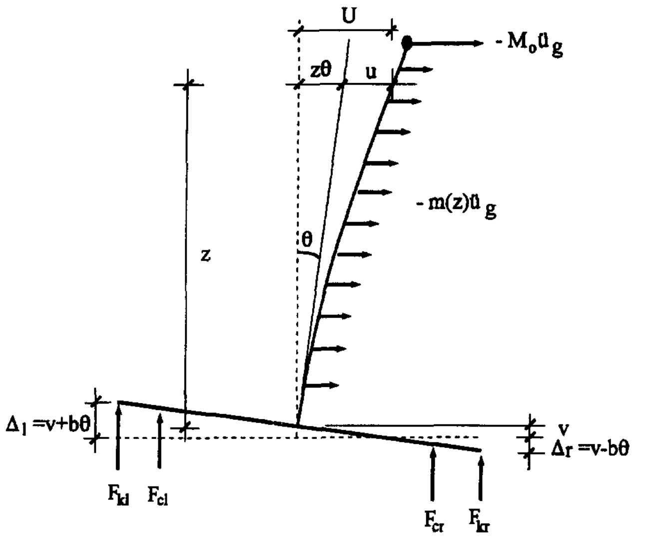

Figure 2 Displacements and forces

is the summation of the tower deflection, $u(x,t)$, and the displacement due to foundation rotation, $z*\theta(t)$. The assumed modes method is employed to approximate the tower deflection, that is,

$$u(x,t) = \sum_{i=1}^{n} \phi_i(x)\, q_i(t) \tag{6}$$

where $\phi_i(x)$ are admissible functions and $q_i(t)$ are generalized co-ordinates. The lowest n-modes of a uniform cantilever beam are selected as admissible functions. Consequently, the system shown in *Figure 2* is characterized by $n + 2$ generalized co-ordinates $q_i(t)$ (i=1, ..., n), $\theta(t)$ and $v(t)$.

Lagrange's equations are employed to derive the equations of motion for the n+2 generalized co-ordinate system shown in *Figure 2*

$$\frac{\mathrm{d}}{\mathrm{d}t}\left(\frac{\partial T}{\partial \dot{q}'_i}\right) - \frac{\partial T}{\partial q'_i} + \frac{\partial V}{\partial q'_i} = Q_i \qquad (i = 1, \ldots, n+2) \tag{7}$$

where T and V denote the kinetic and potential energy, respectively, Q_i are the generalized forces, and q'_i corresponds to $q_i(t)$ (i=1, ..., n), $\theta(t)$ and $v(t)$. The virtual work δW of the nonconservative forces has the following form for any possible virtual generalized co-ordinates

$$\delta W = Q_1 \delta q'_1 + Q_2 \delta q'_2 + \ldots + Q_{n+2}\, \delta q'_{n+2} \tag{8}$$

Three different phases of the response can be identified depending on the contact conditions of the foundation: (a) no foundation uplift; (b) left-side uplifted; and (c) right-side uplifted. The corresponding expressions for the kinetic energy T, potential energy V, and the virtual work of nonconservative forces δW are given in Appendix 1. By substituting T, V and δW given in Appendix 1 into equations (7) and (8), and performing the indicated differentiation for T, V and δW, we obtain the equation of motion for the three different phases in matrix form

$$[M]\{\ddot{x}\} + [C]\{\dot{x}\} + [K]\{x\} = \{Q\} \tag{9}$$

where the matrices and vectors indicated in equation (9) are given by

$$\{x\} = \{q_1(t)\ q_2(t)\ \ldots\ q_N(t)\ \theta(t)\ v(t)\}^T$$

$$\{Q\} = -\ddot{u}_g\{M_1^\phi + M_o\ M_2^\phi + M_o\ \ldots\ M_N^\phi + M_o\ \ M_z + M_o h\ (M_o + M_b + M_f)g/\ddot{u}_g\}^T$$

$$[M] = \begin{bmatrix} M_{11}^\phi + M_o & M_{12}^\phi + M_o & \ldots & M_{1N}^\phi + M_o & M_{1\phi}^z + M_o h & 0 \\ M_{21}^\phi + M_o & M_{22}^\phi + M_o & \ldots & M_{2N}^\phi + M_o & M_{2\phi}^z + M_o h & 0 \\ \vdots & \vdots & & \vdots & \vdots & \vdots \\ M_{N1}^\phi + M_o & M_{N2}^\phi + M_o & \ldots & M_{NN}^\phi + M_o & M_{N\phi}^z + M_o h & 0 \\ M_{\phi 1}^z + M_o h & M_{\phi 2}^z + M_o h & \ldots & M_{\phi N}^z + M_o h & M_z^z + M_o h^2 + I_f & 0 \\ 0 & 0 & \ldots & 0 & 0 & M_o + M_b + M_f \end{bmatrix}$$

$$[K] = \begin{bmatrix} K_{11}^\phi & K_{12}^\phi & \ldots & K_{1N}^\phi & 0 & 0 \\ K_{21}^\phi & K_{22}^\phi & \ldots & K_{2N}^\phi & 0 & 0 \\ \vdots & \vdots & & \vdots & \vdots & \vdots \\ K_{N1}^\phi & K_{N2}^\phi & \ldots & K_{NN}^\phi & 0 & 0 \\ 0 & 0 & \ldots & 0 & \epsilon_1 k_v b^2 & \epsilon_2 k_v b \\ 0 & 0 & \ldots & 0 & \epsilon_2 k_v b & \epsilon_1 k_v \end{bmatrix}$$

and

$$[C] = \begin{bmatrix} C_{11}^\phi & C_{12}^\phi & \ldots & C_{1N}^\phi & 0 & 0 \\ C_{21}^\phi & C_{22}^\phi & \ldots & C_{2N}^\phi & 0 & 0 \\ \vdots & \vdots & & \vdots & \vdots & \vdots \\ C_{N1}^\phi & C_{N2}^\phi & \ldots & C_{NN}^\phi & 0 & 0 \\ 0 & 0 & \ldots & 0 & \epsilon_1 c_v b^2 & \epsilon_2 c_v b \\ 0 & 0 & \ldots & 0 & \epsilon_2 c_v b & \epsilon_1 c_v \end{bmatrix}$$

The parameters of ϵ_1, ϵ_2 in matrices $[K]$ and $[C]$ take the values

$$\epsilon_1 = \begin{cases} 2 & \text{no uplift} \\ 1 & \text{uplifted} \end{cases}$$

$$\epsilon_2 = \begin{cases} 1 & \text{right-side uplifted} \\ 0 & \text{no uplift} \\ -1 & \text{left-side uplifted} \end{cases}$$

The expressions for evaluating the coefficients of the stiffness and mass matrices are given in Appendix 2.

It should be noted that the damping matrix $[C]$ consists of two parts

$$[C] = \begin{bmatrix} [C]_t & 0 \\ 0 & 0 \end{bmatrix} + \begin{bmatrix} 0 & 0 \\ 0 & [C]_s \end{bmatrix} \tag{10}$$

where the damping matrices $[C]_t$ and $[C]_s$ express damping of the tower and the soil, respectively. If the damping coefficient per unit length $c(z)$ along the height of the tower is known, one can calculate $[C]_t$ through the expressions given in Appendix 2. In general the matrix $[C]_t$ is calculated through the expression[23,24]

$$[C]_t = [M] \sum_i a_i([M]^{-1}[K])^i \tag{11}$$

where the parameters a_i are related to damping ratios ξ_i, and the circular natural frequency ω_i as given by

$$\xi_n = \frac{1}{2\omega_n} \sum_i a_i \omega_n^{2i} \tag{12}$$

Equation (12) can be used to determine the constants a_i for selected modal damping ratios. The matrix $[C]_s$ is formed by using the soil damping coefficient given by equation (3).

3. Numerical treatment

The equations of motion comprise a system of piecewise-linear second-order differential equations that can be solved with the aid of several available numerical methods, see Spyrakos[23] and Bathe[25]. Newmark's method has been employed to perform the numerical integration. In this work, δ is selected as equal to 0.5 and α = 0.25. The $a_i(i = 0, 1, \ldots, 7)$ in Newmark's method are given by[26]

$$a_0 = \frac{1}{\alpha \Delta t^2} \quad a_1 = \frac{\delta}{\alpha \Delta t} \quad a_2 = \frac{1}{\alpha \Delta t} \quad a_3 = \frac{1}{2\alpha} - 1$$

$$a_4 = \frac{\delta}{\alpha} - 1 \quad a_5 = \frac{\Delta t}{2}\left(\frac{\delta}{\alpha} - 2\right) \quad a_6 = \Delta t(1-\delta) \quad a_7 = \delta \Delta t \quad (13)$$

The selection of time step Δt is of critical importance for solution accuracy. More detailed discussions and guidelines on selecting a time step Δt can be found elsewhere[23,25]. As a widely accepted rule for multi-degree-of-freedom systems, one can select $\Delta t = \min \{T_c/20/\pi, T_E/20/\pi\}$, where T_c is a critical vibration period of the structure, and T_E is the smallest period of the excitation. For the Briones Dam tower subjected to the 1940 El-Centro N-S earthquake ground excitation (see Section 4 for detail parameters) the maximum displacement at the top and the maximum moment and shear force at the base for several selected time steps are plotted in *Figure 3*. From this plot, one can conclude that a time step of 0.0005 s is suitable, it provides practically identical results to when a smaller time step of 0.00001 s is used. Thus, a time step of 0.0005 s has been used for all calculations in the following parametric studies.

Since the accuracy of the solution depends on the number of eigen-modes included in the formulation, a comparative study was carried out. It showed that a five-mode formulation is sufficient to determine the seismic response[21].

4. Numerical examples

The 1940 El-Centro N-S earthquake ground motion is selected as the excitation. The maximum acceleration amplitude of this ground motion is about 0.33 *g*. In order to induce uplift, the amplitude of the ground motion has been amplified by a factor of two, an order of magnitude that has been recorded in several seismic motions.

The Briones Dam Intake-Outlet tower[26] located east of the San Francisco Bay is studied as an illustrative example. The radius of the tower varies linearly along its height. Its sectional constants are: top inner radius = 1.52 m, top outer radius = 1.86 m, bottom inner radius = 3.05 m, and bottom outer radius = 3.45 m. The height of the tower is approximately 70.10 m and the radius of the foundation is 9.14 m.

The tower is a reinforced concrete structure. In this study, it is assumed to be homogeneous, isotropic, linear elastic with Young's modulus E = 31000 MPa, and unit weight = 2483 kg/m^3. The damping ratio for each mode, i.e., $\xi_i(i = 1, \ldots, 5)$ in equation (12) is equal to 0.05. The material properties of the supporting soil are: mass density = 2644 kg/m^3, shear modulus G = 245.6 MPa, Poisson's ratio = 1/3, and the shear wave velocity = 304.8 m/s.

4.1. Comparison of tower models

Different idealized models of the towers have been developed, depending on whether or not the variation of the tower cross-section, the presence of any mass at the top, and the mass of foundation block are included in the analysis. Four different models are considered. In model I, the tower is modelled as a uniform beam; no top and foundation mass are included. The midpoint sectional constants are used, i.e., inner radius = 2.29 m and outer radius = 2.66 m. In model II, the tower is idealized as a tapered beam with no top mass and no foundation mass. In contrast to model II, model III includes the foundation mass. In model IV, in addition to the foundation mass, the top mass, which is 1/10 of the total tower body mass, is also included.

The results presented in *Figure 4* and *Table 1* demonstrate several differences among the models subjected to the same excitation. *Figure 4a* shows the seismic response

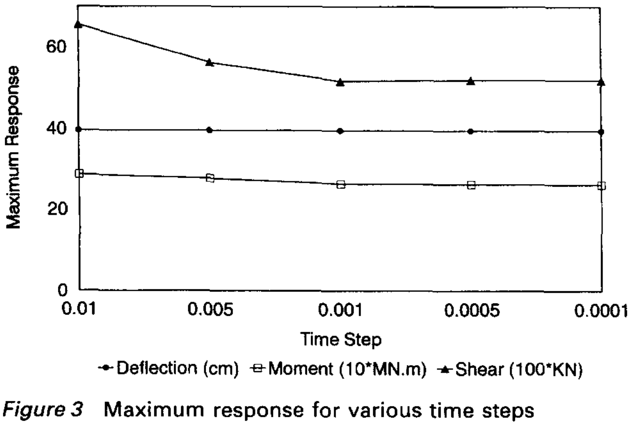

Figure 3 Maximum response for various time steps

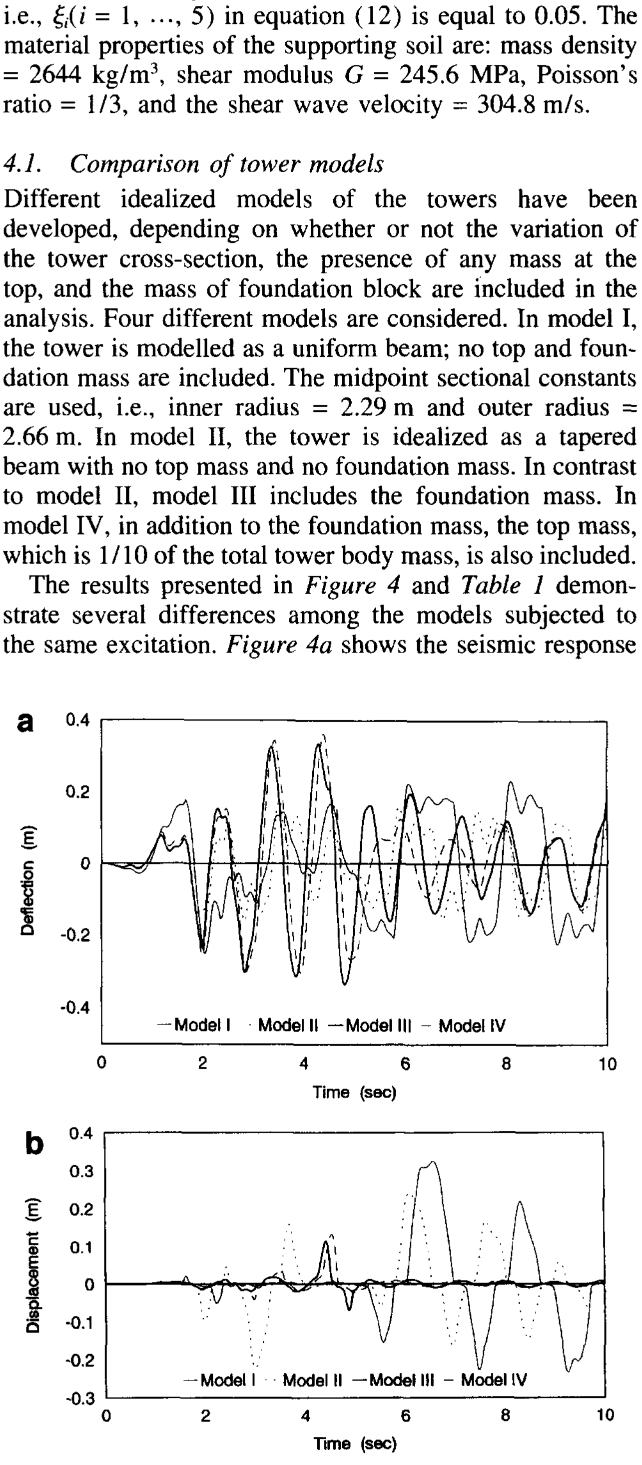

Figure 4 Comparison of tower models. (a) deflection; (b) displacement due to rotation

Table 1 Seismic response of different models

	Model I	Model II	Model III	Model IV
Deflection (cm)	25.14	19.10	33.73	36.39
Moment (MN.m)				
Shear (MN)	96.39	105.76	261.88	234.44
	4.06	5.48	5.20	9.59

of the top deflection of the tower for the four models. *Figure 4b* depicts the seismic response of the top displacement due to the rotation of the foundation. The maximum top deflection, base moment, and base shear force are given in *Table 1*. It is clear from *Figure 4* and *Table 1* that the models respond quite differently. Specifically, from the seismic response one can classify the response of the tower in two categories. In the first category, the models exclude the foundation in the analysis, whereas in the second category the foundation is included. For the selected ground excitation, uplift was observed only in the models of the first category. This clearly demonstrates the effect of the foundation mass on the system's response. Comparing models I and II, it can be seen that tapering decreases the deflection at the top and increases the base moment and shear. The absence of uplift in models III and IV leads to increased deflection at the top as compared to models I and II. Overall, there is an increase of the base moment and shear for models of the second category. The presence of the top mass in model IV increases the deflection and decreases the moment as compared to model III.

4.2. *Effect of soil stiffness*

Six representative types of soil are compared. The shear moduli for selected soil conditions are: G = 34.5, 68.9, 103.4, 137.9, 245.6 and 344.7 MPa. Note that G = 34.5 MPa corresponds to a soft soil, while G = 344.7 MPa characterizes hard rock-like soil strata. The shear modulus of 245.6 MPa is computed from the soil properties of the Briones Dam tower location. In evaluating the effects of soil stiffness, the tower is modelled as the tapered beam with no top operation unit and with the foundation mass included. Two cases of height-width (H/B) ratios are considered. The first one with H/B = 7.7 corresponds to the geometry of the Briones Dam tower, and the other with H/B = 20 to a slender tower. *Figure 5* shows the seismic response of the tower for the representative soil stiffnesses. It should be noted that the effects of soil stiffness are significant when H/B = 7.7. Overall the seismic response increases with increasing soil stiffness, especially for the moment and shear. Both moment and shear almost double when the soil changes from soft soil to hard rock. When the tower becomes more slender, however, the effect of soil stiffness on the seismic response decreases. For the tower with H/B = 20, deflection, moment and shear remain practically the same regardless of the soil conditions. It should be noted that the displacement due to foundation rotation decreases substantially when the soil becomes harder, which also results in similar behaviour for the top displacement.

4.3. *Effects of height-width ratio*

In this section, the seismic response of the tower is evaluated for various ratios of tower height to foundation width. The same tower model used in the previous section is used

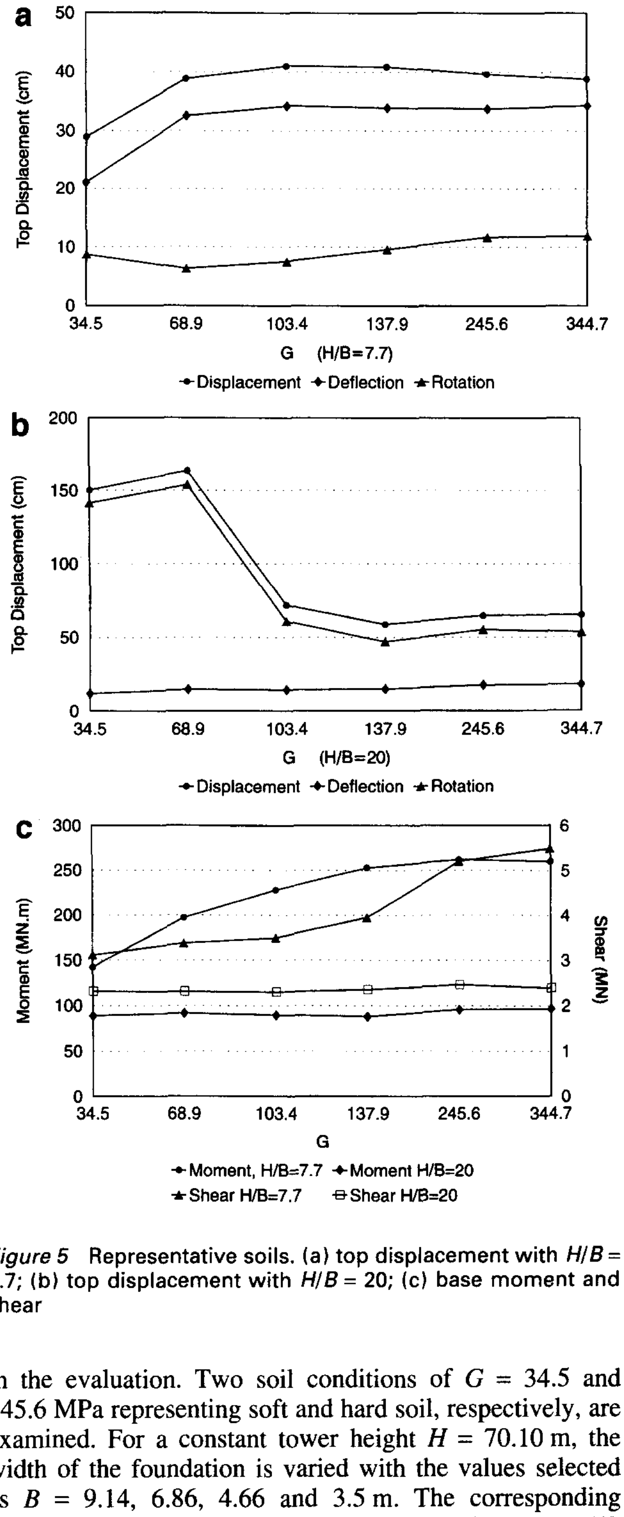

Figure 5 Representative soils. (a) top displacement with H/B = 7.7; (b) top displacement with H/B = 20; (c) base moment and shear

in the evaluation. Two soil conditions of G = 34.5 and 245.6 MPa representing soft and hard soil, respectively, are examined. For a constant tower height H = 70.10 m, the width of the foundation is varied with the values selected as B = 9.14, 6.86, 4.66 and 3.5 m. The corresponding height-width ratios are H/B = 7.7, 10, 15 and 20. The H/B ratio of 7.7 corresponds to the Briones Dam tower. The seismic response for the selected H/B ratios is plotted in *Figure 6*. It is apparent that the H/B ratio has a significant effect on the seismic response. It is observed that the wider the foundation, the larger the maximum seismic response. Notice, however, that the foundation rotation and displacement decrease for increasing foundation dimensions. It is also clear from *Figure 6* that the H/B ratios play a more important role for the harder soil than for the softer soil. For the harder soil with G = 245.6 MPa, when the H/B ratio changed from 20 to 7.7, the moment is trippled and the shear is doubled, while for the soft soil with G = 34.5 MPa, the increment for moment is less than 100% and

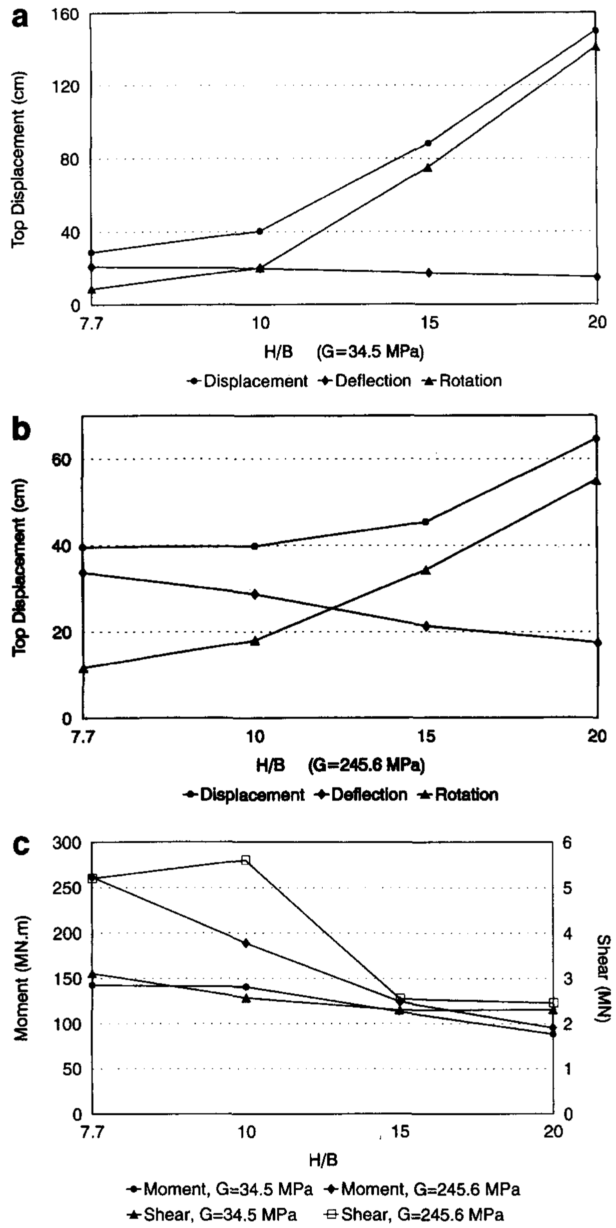

Figure 6 Role of *H/B* ratios. (a) top displacement (G = 34.5 MPa); (b) top displacement (G = 245.6 MPa); (c) base moment and shear

for the shear the increment is less than 40%. The result clearly demonstrates the important role that the H/B ratio plays in the seismic response of a tower. It can also be observed that the maximum seismic response can be decreased by reducing the size of the foundation. However, a tower with narrow foundations tends to overturn more easily as can be seen from *Figure 6*. Thus, the dimension of a foundation should be decided by considering both the strength and stability requirements[27].

4.4. *Effects of foundation uplift*

The influence of foundation uplift on the seismic response is studied in this section. The tower model with no top unit mass but with foundation mass, as in the previous sections, is used. Altogether, eight cases are investigated for the effects of foundation uplift. The cases are generated by combining two soil conditions and four H/B ratios. The results are given in *Table 2* and *Figure 7*.

The figures are drawn for the special case of the Briones Dam tower with G = 34.5 MPa and H/B = 7.7. The deflection of the tower is presented in *Figure 7a*, and the foundation rotation is shown in *Figure 7b*. As shown in *Figure 7b*, the foundation rotation with uplift is much greater than when uplift is restrained. This phenomena is attributed to the fact that after uplift the foundation rotation increases greatly. The top deflection with uplift is less than that under complete bonding at the soil–foundation interface (see *Figure 7a*).

Table 2 lists the results of the seismic response for the eight cases. They demonstrate that foundation uplift greatly affects the seismic response of the tower. Observations that can be drawn from *Table 2* include: firstly, the influence of foundation uplift on hard soil is greater than on soft soil; secondly, the base moment decreases when uplift is permitted and an increase in the base shear is observed for hard soil; and finally, the influences of foundation uplift on deflection and moment increase with increasing H/B ratio. However, its effect on foundation rotation and shear decreases with increasing H/B ratio.

In conclusion, uplift affects the seismic response of the tower in a manner that is not necessarily beneficial to the system's behaviour under seismic loads, since it increases some seismic responses while it decreases other seismic responses.

5. Conclusions

The procedure developed in this work examines the seismic response of towers. It incorporates aspects regarding tower

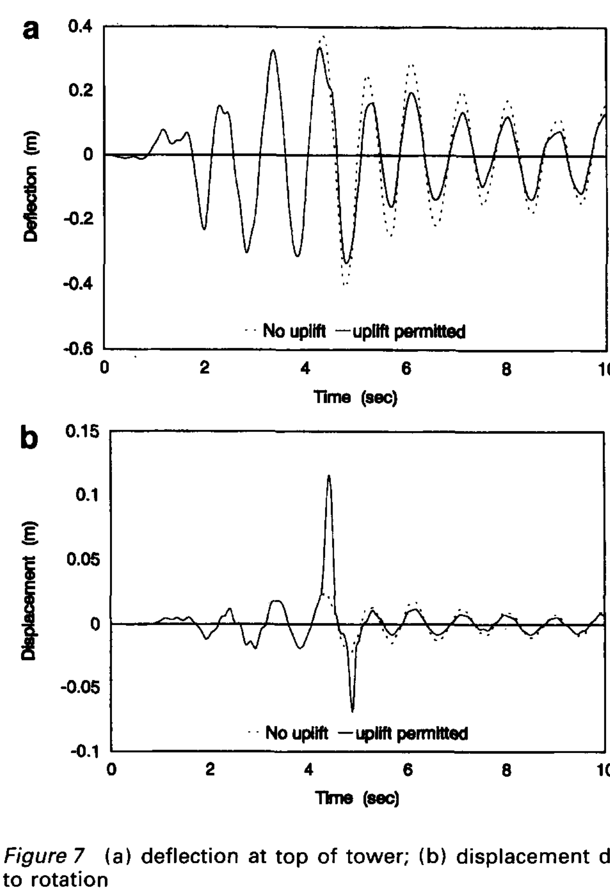

Figure 7 (a) deflection at top of tower; (b) displacement due to rotation

Table 2 Maximum seismic response for bonded and unbonded conditions

G (MPa)	*H/B*	Bond conditions	Displ. (cm)	Deflection (cm)	Displ. due to rotation (cm)	Moment (MN.m)	Shear (MN)
245.6	7.7	Uplifted	39.55	33.73	11.68	261.88	5.20
		No uplift	43.02	40.81	2.47	275.76	3.63
	10	Uplifted	39.79	28.68	18.01	189.17	5.60
		No uplift	43.75	38.61	5.26	251.94	3.57
	15	Uplifted	45.36	21.25	34.16	124.17	2.55
		No uplift	42.38	29.46	13.31	197.88	2.79
	20	Uplifted	64.70	17.48	55.15	95.56	2.46
		No uplift	51.19	24.34	27.52	162.5	2.43
34.5	7.7	Uplifted	No uplift occurs				
		No uplift	28.94	20.98	8.70	142.5	3.11
	10	Uplifted	No uplift occurs				
		No uplift	40.31	19.99	20.34	140.83	2.57
	15	Uplifted	88.28	17.33	75.11	113.13	2.30
		No uplift	86.23	18.92	67.65	137.43	2.30
	20	Uplifted	150.2	14.88	141.32	88.61	2.32
		No uplift	152.1	18.02	137.64	118.96	2.32

geometry, the presence of a massive foundation, and top operating unit as well as nonlinearity from soil–foundation partial separation. Yet, it is simple enough to maintain a feel for the physical parameters and can be used for preliminary analysis and design of a rather complex tower system. For a representative tower and a selected earthquake ground motion, the conclusions of these parametric studies can be summarized as follows.

In idealizing a tower structure, attention should be paid in developing an appropriate model, especially for the mass distributed at the higher parts of the tower since its effect on the seismic response is much greater than that of the mass distributed close to the foundation. Also, if uplift is allowed, the foundation mass will have a significant influence on the seismic response, and should be included in the analysis.

Soil stiffness can play an important role in the seismic response of towers. The seismic response of a tower with wide foundation is more significantly affected by the soil stiffness. However, increasing soil stiffness can reduce the foundation rotation substantially even for a tower with a narrow foundation. The behaviour of a tower on stiff soil is very similar to that of a system supported on a rigid base.

The slenderness ratio greatly affects the seismic response. This effect is more profound for hard soil rather than soft soil. For a given soil stiffness and height, a tower with a wider foundation exhibits a much more severe seismic force response than a tower with a more narrow foundation. However, the behaviour of the foundation rotation is the reverse. This implies that in order to reduce the seismic stresses response in towers, narrow foundations could be used. However, towers with narrow foundations tend to produce larger foundation rotation and thus the likelihood of overturning will increase.

Uplift can have a significant effect on the seismic response. This study demonstrates that the effects of uplift can lead not only to a reduction of deflections and moments but also to an increase in base shear and foundation rotation. The effects of harder soil are more profound than those of softer soil. Uplift affects the seismic response of the tower differently for various height/width ratios. The observations from the limited parametric studies clearly indicate that the notion that uplift benefits the system's response is not necessarily always correct and should be given proper attention.

The conclusions are based on the particular tower, a specific ground excitation and parametric studies. In order to arrive at general conclusions and develop design equations that account for foundation uplift of tower structures, further parametric studies are needed.

Acknowledgments

The financial support (DACN39-92-c-0061) of the Structures Division (CEWES-SS-A) of U.S. Army Waterways Experiment Station that made this study possible is gratefully acknowledged.

References

1 Ishiyama, Y. 'Review and discussion on overturning of bodies by earthquake motions', BRI Research Paper 85, Japanese Ministry of Construction, 1980
2 Milne, J. 'Experiments in observational seismology', *Trans. Seismol. Soc. Jap.* 1881, **3**, 42–64
3 Housner, G. W. 'The behavior of inverted pendulum structures during earthquakes', *Bull. Seismol. Soc. Am.* 1963, **53** (2), 503–417
4 Yim, C.-S., Chopra, A. K. and Penzien, J. 'Rocking response of rigid blocks to earthquakes', *Earthquake Engng Struct. Dyn.* 1980, **8**, 565–587
5 Spanos, P. D. and Koh, A.-S. 'Stochastic response of rigid blocks on flexible foundation', *Proc. Eighth Int. Conf. Struct. Mech. in Reactor Tech.* (SMiRT-8), 1985, pp. 327–332
6 Spanos, P. D. and Koh, A.-S. 'Rocking of rigid blocks due to harmonic shaking', *J. Engng. Mech., ASCE* 1984, **110** (11), 1627–1642
7 Housner, G. W. 'Dynamic pressures on accelerated fluid containers', *Bull. Seism. Soc. Am.* 1957, **47**, 15–35
8 Luco, J. E. 'Soil-structure interaction effects on the seismic response of tall chimneys', *Soil Dyn. Earthquake Engng* 1986, **5**, 170–177
9 Wolf, J. P. '*Dynamic soil-structure interaction*', Prentice-Hall, Englewood Cliffs, NJ, 1984
10 Spyrakos, C. C., Patel, P. N. and Kokkinos, F. T. 'Assessment of computational practices in dynamic soil-structure interaction', *J. Comput. Civ. Engng* 1989, **3** (2), 143–157
11 Spyrakos, C. C. 'Dynamic behavior of foundations in bilateral and unilateral contact', *Shock Vibr. Digest* 1988, **20** (8), 561–587
12 Spyrakos, C. C. and Antes, H. 'Time domain boundary element method approaches in elastodynamics: a comparative study', *Comput. Struct.* 1986, **24**, 529–535
13 Spyrakos, C. C. '*Boundary element techniques in geomechanics*' (Eds C. D. Manolis and T. G. Davies) CMP-Elsevier, New York, 1993, Chapter 5
14 Antes, H. and Spyrakos, C. C. 'Dynamic analysis of massive block to transient Raleigh waves', *Proc., ASCE Structures Congress*, Volume on dynamics of structures, pp. 512–518, 1987
15 Psycharis, I. N. and Jennings, P. 'Rocking of slender rigid bodies allowed to uplift', *Earthquake Engng Struct. Dyn.* 1983, **11**, 57–76
16 Chopra, A. K. and Yim, C.-S. 'Simplified earthquake analysis of

structures with foundation uplift', *J. Struct. Engng ASCE* 1985, **111** (4), 906–930
17 Yim, C.-S. and Chopra, A. K. 'Simplified earthquake analysis of multistory structures with foundation uplift', *J. Struct. Engng, ASCE*, 1985, **111** (12), 2708–2731
18 Al-Deghaither, S. E. 'Seismic response of bridge piers including soil-structure interaction', Masters Thesis, College of Engineering of West Virginia University, Morgantown, WV, 1988
19 Patel, P. N. and Spyrakos, C. C. 'Time domain BEM-FEM seismic analysis including basement lift-off', *Engng Struct.* 1990, **12** (7), 195–207
20 Patel, P. N. and Spyrakos, C. C. 'Uplifting-sliding response of flexible structures to seismic loads', *Engng Anal. with Boundary Elements* 1991, **8** (4), 185–191
21 Xu, C. J. 'Seismic analysis of towers and intake-outlet towers including effects of foundation uplift', MS Thesis submitted to the College of Engineering of West Virginia University, Morgantown, WV, 1992
22 Psycharis, I. N. 'Effect of base uplift on dynamic response of SDOF structure', *J. Struct. Engng, ASCE* 1991, **117** (3), 733–754
23 Spyrakos, C. C. '*Finite element modeling in engineering practice*', West Virginia University Press, Morgantown, WV, 1994
24 Paz, M. '*Structural dynamics: theory and computation*' (3rd edn) Van Nostrand Reinhold, New York, 1991
25 Bathe, K.-J. '*Finite element procedures in engineering analysis*', Prentice-Hall, Englewood Cliffs, NJ, 1982
26 Goyal, A. and Chopra, A. K. 'Hydrodynamic and foundation effects in dynamics of intake towers: earthquake responses', *J. Struct. Engng, ASCE* 1989, **115** (6), 1386–1394
27 Kiger, S., Spyrakos, C. C. and Xu, C. J. 'Overturning stability of flexible intake/outlet towers', Final Report submitted to Waterways Experiment Station, West Virginia University, Morgantown, WV, 1993

Appendix 1

Kinetic energy

$$
\begin{aligned}
T &= \frac{1}{2}\int_0^h m(z)\,(\dot{u}+z\dot{\theta})^2\,\mathrm{d}z + \frac{1}{2}M_o(\dot{u}|_{z=h}+h\dot{\theta})^2 \\
&\quad + \frac{1}{2}(M_o+M_b+M_f)\,\dot{v}^2 + \frac{1}{2}I_f\,\dot{\theta}^2 \\
&= \frac{1}{2}\int_0^h m(z)\left(\sum_{i=1}^{N}\phi_i(z)\dot{q}_i(t) + z\dot{\theta}\right)^2 \mathrm{d}z \\
&\quad + \frac{1}{2}M_o\left(\sum_{i=1}^{N}\dot{q}_i(t)+h\dot{\theta}\right)^2 + \frac{1}{2}(M_o+M_b+M_f)\dot{v}^2 + \frac{1}{2}I_f\dot{\theta}^2 \\
&= \frac{1}{2}\sum_{i=1,j=1}^{N}\left(\int_0^h m(z)\phi_i(z)\phi_j(z)\mathrm{d}z+M_o\right)\dot{q}_i(t)\dot{q}_j(t) \\
&\quad + \sum_{i=1}^{N}\left(\int_0^h z\,m(z)\phi_i(z)\,\mathrm{d}z+M_oh\right)\dot{q}_i(t)\dot{\theta} \\
&\quad + \frac{1}{2}\left(\int_0^h m(z)z^2\,\mathrm{d}z+M_oh^2\right)\dot{\theta}^2 + \frac{1}{2}(M_o+M_b+M_f)\dot{v}^2 \\
&\quad + \frac{1}{2}I_f\,\dot{\theta}^2
\end{aligned}
$$

Potential energy

$$
\begin{aligned}
V &= \frac{1}{1}\int_0^h EI(z)\left(\frac{\mathrm{d}^2u}{\mathrm{d}z^2}\right)^2 \mathrm{d}z + (M_o+M_b+M_f)gv \\
&\quad + \begin{cases} \frac{1}{2}k_v(v+b\theta)^2 & \text{right-side uplifted} \\ \frac{1}{2}k_v(v+b\theta)^2 + \frac{1}{2}k_v(v-b\theta)^2 & \text{no uplift} \\ \frac{1}{2}k_v(v-b\theta)^2 & \text{left-side uplifted} \end{cases} \\
&= \frac{1}{2}\int_0^h EI(z)\left(\sum_{i=1}^{N}\frac{\mathrm{d}^2\phi}{dz^2}q_i(t)\right)^2 \mathrm{d}z + (M_o+M_b+M_f)gv \\
&\quad + \frac{1}{2}\epsilon_1k_vv^2 + \epsilon_2k_vb\theta + \frac{1}{2}\epsilon_1k_vb^2\theta^2 \\
&= \frac{1}{2}\sum_{i,j=1}^{N}\int_0^h EI(z)\frac{\mathrm{d}^2\phi_i(z)}{\mathrm{d}z^2}\frac{\mathrm{d}^2\phi_j(z)}{\mathrm{d}z^2}\,\mathrm{d}z\,q_i(t)q_j(t) \\
&\quad + (M_o+M_b+M_f)\,gv + \frac{1}{2}\epsilon_1k_vv^2 + \epsilon_2k_vb\theta + \frac{1}{2}\epsilon_1k_vb^2\theta^2
\end{aligned}
$$

The notation of ϵ_1, ϵ_2 is given in the text.

Virtual work

$$
\begin{aligned}
\delta W &= -\int_0^h m(z)\ddot{u}_g(\delta u+z\delta\theta)\,\mathrm{d}z \\
&\quad - M_o\ddot{u}_g(\delta u|_{z=h}+h\delta\theta) \\
&\quad - \int_0^h c(z)\,\dot{u}\delta u\mathrm{d}z \\
&\quad + \begin{cases} c_v(\dot{v}+b\dot{\theta})\,(\delta v+b\delta\theta) & \text{right-side uplifted} \\ c_v(\dot{v}+b\dot{\theta})\,(\delta v+b\delta\theta) + c_v(\dot{v}+b\dot{\theta})(\delta v-b\delta\theta) & \text{no uplift} \\ c_v(\dot{v}-b\dot{\theta})\,(\delta v-b\delta\theta) & \text{left-side uplifted} \end{cases} \\
&= -\int_0^h m(z)\,\ddot{u}_g\left(\sum_{i=1}^{N}\phi_i(z)\delta q_i(t) + z\delta\theta\right)\mathrm{d}z - M_o\ddot{u}_g\left(\sum_{i=1}^{N}\delta q_i(t)+h\delta\theta\right) \\
&\quad - \left(\int_0^h c(z)\sum_{i=1}^{N}\phi_i(z)\sum_{j=1}^{N}\phi_j(z)\,\mathrm{d}z\right)\dot{q}_i(t)\delta q_j(t) \\
&\quad + \epsilon_1c_v(\dot{v}\delta\theta+b^2\dot{\theta}\delta v) + \epsilon_2c_vb(\dot{v}\delta\theta+\dot{\theta}\delta v) \\
&= -\sum_{i=1}^{N}\ddot{u}_g\left(\int_0^h m(z)\,\phi_i(z)\,\mathrm{d}z+M_o\right)\delta q_i(t) - \ddot{u}_g\left(\int_0^h zm(z)\,\mathrm{d}z+M_oh\right)\delta\theta \\
&\quad - \sum_{i=1,j=1}^{N}\int_0^h c(z)\,\phi_i(z)\phi_j(z)\,\mathrm{d}z\,\dot{q}_i(t)\,\delta q_j(t) \\
&\quad + \epsilon_1c_v(\dot{v}\delta\theta+b^2\dot{\theta}\delta v) + \epsilon_2c_vb(\dot{v}\delta\theta+\dot{\theta}\delta v)
\end{aligned}
$$

Appendix 2

$$M_{ij}^{\phi} = \int_0^h m(z)\phi_i(z)\phi_j(z)\mathrm{d}z$$

$$C_{ij}^{\phi} = \int_0^h c(z)\phi_i(z)\phi_j(z)\mathrm{d}z$$

$$K_{ij}^{\phi} = \int_0^h EI(z)\frac{\mathrm{d}^2\phi_i(z)}{\mathrm{d}z^2}\frac{\mathrm{d}^2\phi_j(z)}{\mathrm{d}z^2}\,\mathrm{d}z$$

$$M_{i\phi}^{z} = M_{\phi i}^{z} = \int_0^h zm(z)\phi_i(z)\mathrm{d}z \qquad M_z^2 = \int_0^h z^2m(z)\mathrm{d}z$$

$$M_i^{\phi} = \int_0^h m(z)\phi_i(z)\mathrm{d}z \qquad M_z = \int_0^h zm(z)\mathrm{d}z$$